



Crystallization behaviors of poly(ethylene terephthalate) (PET) with monosilane isobutyl-polyhedral oligomeric silsesquioxanes (POSS)

Xian Zhang¹, Shicheng Zhao¹, Mohamed Gamal Mohamed², Shiao-Wei Kuo^{2,*}, and Zhong Xin^{1,*} 

¹ Shanghai Key Laboratory of Multiphase Materials Chemical Engineering, Department of Product Engineering, East China University of Science and Technology, Shanghai 200237, People's Republic of China

² Department of Materials and Optoelectronic Science, National Sun Yat-Sen University, Kaohsiung 804, Taiwan

Received: 8 May 2020

Accepted: 21 June 2020

Published online:
13 July 2020

© Springer Science+Business Media, LLC, part of Springer Nature 2020

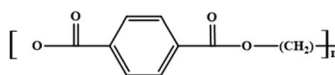
ABSTRACT

The crystallization behaviors of poly(ethylene terephthalate) (PET) with monosilane isobutyl-polyhedral oligomeric silsesquioxanes (POSS) were investigated in detail. It is observed that POSS acts as an effective nucleating agent under appropriate concentration in the PET system. Polarized optical microscopy (POM) results showed that POSS improved the nucleation density of PET. Besides, the transmission electron microscopy (TEM) observation demonstrated POSS dispersed mostly at the nanometer scale throughout the PET matrix. The crystal structures of POSS and PET/POSS were analyzed using wide-angle X-ray diffraction (WAXD). Moreover, non-isothermal crystallization kinetics of PET and PET/POSS were studied using Mo's method. The PET/POSS system demonstrated the lower value of $F(T)$ than pure PET, indicating that the lower cooling rate was required to attain a specified relative crystallinity for the system. The comparison of the crystallization activation energy (ΔE) showed that the POSS nanoparticles improved the crystallization of PET through an acceleration of the nucleation process. Furthermore, the isothermal crystallization behaviors were also investigated using classic Avrami method. Overall, POSS can act as a nucleating agent and greatly improve the crystallization of PET through accelerating the nucleation process.

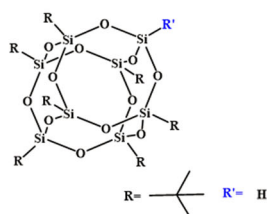
Address correspondence to E-mail: kuosw@faculty.nsysu.edu.tw; xzh@ecust.edu.cn

GRAPHIC ABSTRACT

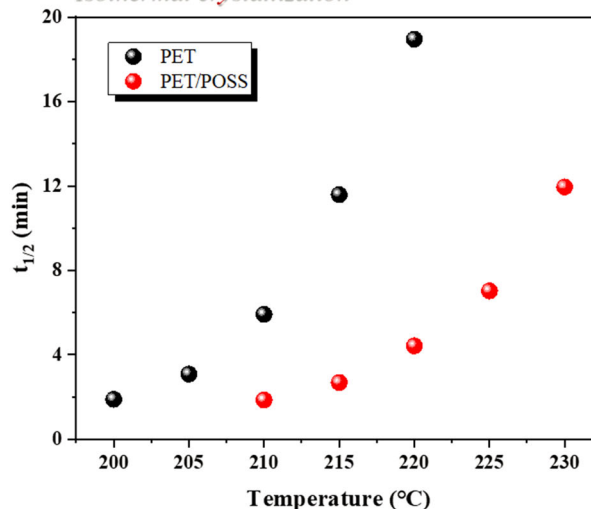
PET



POSS



Isothermal crystallization



Introduction

Poly(ethylene terephthalate) (PET) is extensively used in many fields owing to its rather versatile properties. As an intrinsic semicrystalline polymer, its properties largely depend on crystallization behaviors, which can control the microstructure formation of polymer and greatly affect the performance of final product. As we all know, the introduction of foreign substances into the polymer can control its properties, such as effectively changing the crystal structure, accelerating the crystallization process, and reducing the crystal size, thereby improving the processing and mechanical properties of PET. So far, there have been many studies on enhancing crystallization behaviors of PET [1–4]. Polyhedral oligomeric silsesquioxanes (POSS) are a hybrid nanoparticle, which is a family of novel nanofillers containing rigid Si inorganic cores modified by organic groups [5]. More than 100 different POSS molecules with different organic functional groups are commercially available. The incorporation of POSS nanoparticles within polymers to form organic/inorganic hybrid materials is a particularly active field of research in industry and academia

because POSS have well-defined structure, zero dimensionality, monodisperse molecular weight, ultra-low dielectric constant, high temperature-stability, and greater design flexibility relative to the conventional fillers (such as clay, carbon nanotube, graphene) [6, 7]. POSS have become the focus of many researchers in processing various polymers through copolymerization, grafting, and conventional mixing [8–10].

It is interesting to note that POSS can also behave as a nucleating agent for the semicrystalline polymers and accelerate the crystallization process in some cases [11–14]. Many kinds of research have been done to investigate the effect of POSS with different functional groups on the properties of PET [15–17]. A lot of POSS has been reported to have positive effect on the crystallization behaviors of PET [17, 18]. However, the POSS nanoparticles with different functional groups might have different effects on crystallization behaviors of the polymers. To our knowledge, the crystallization behaviors of PET/monosilane isobutyl-POSS nanocomposites have not been reported so far in the literature.

Therefore, we prepared the PET nanocomposites with different contents of POSS in this work. The

crystallization behaviors of the samples were investigated. The dispersion of POSS in the PET matrix was studied using transmission electron microscopy (TEM) and wide-angle X-ray diffraction (WAXD). The differential scanning calorimetry (DSC) and polarized optical microscopy (POM) were used to study the crystallization behaviors of the samples. Moreover, the non-isothermal crystallization kinetics of PET/POSS nanocomposites were studied using Mo's model and the isothermal crystallization behaviors were also investigated using the classic Avrami method. It is expected that the results reported herein are of interest and importance in the fields of polymer crystallization from both the fundamental and practical viewpoints.

Experimental

Materials

In this study, the PET pellets were provided with intrinsic viscosity of 0.5 dL g^{-1} by Jingming Chemical Co., Ltd (China). The polyhedral oligomeric silsesquioxanes (POSS) nanoparticles were supplied by Dongda Teng Technology Co., Ltd. The molecular structure of PET and POSS studied here is shown in Fig. 1. 1,1,2,2-Tetrachloroethane and phenol were purchased from Sigma-Aldrich. All chemicals were

of analytical grade and used as received without further purification.

Preparation of PET/POSS nanocomposites

5 g of PET with various mass fractions of POSS (0%, 0.5%, 1%, 3%, 5%, and 7%, named as pure PET, PET/POSS-0.5, PET/POSS-1, PET/POSS-3, PET/POSS-5, and PET/POSS-7) was dissolved in 20 mL of solvent mixture of 1,1,2,2-tetrachloroethane/phenol mixture (50/50 w/w). The mixture was stirred overnight at $80 \text{ }^\circ\text{C}$. After that, 3 mL of the mixture was dropped onto an aluminum plate, and the solvent was evaporated in the room temperature. All the samples were dried in a vacuum oven at $120 \text{ }^\circ\text{C}$ for 24 h before further characterization.

Characterizations

Differential scanning calorimeter (DSC) was performed using a TA-Q20 instrument operated at a scan rate of $20 \text{ }^\circ\text{C min}^{-1}$ under the protection of the nitrogen atmosphere (60 mL min^{-1}), which acted as an inert gas and prevented sample degradation. The samples (3–5 mg) were sealed in the aluminum pans during the experiment. Also, the temperature was calibrated by using indium as a standard medium before the measurements in the range of 30 to $300 \text{ }^\circ\text{C}$. During the experiment, the samples were heated to $280 \text{ }^\circ\text{C}$ and kept at this temperature for 5 min to eliminate thermal history (different manufacturing and storage conditions) and then cooled to $50 \text{ }^\circ\text{C}$ at a cooling rate of $20 \text{ }^\circ\text{C min}^{-1}$. In the non-isothermal process, the samples were cooled from 280 to $50 \text{ }^\circ\text{C}$ at cooling rates (Φ) of 2.5, 5, 10, 15, and $20 \text{ }^\circ\text{C}\cdot\text{min}^{-1}$. The exothermal curves of heat flow as a function of time and temperature were recorded. In the isothermal process, the samples were quenched from $280 \text{ }^\circ\text{C}$ to predetermined crystallization temperature at the cooling rate (Φ) of $10 \text{ }^\circ\text{C min}^{-1}$ and kept it until complete crystallization. The exothermal curves of heat flow as a function of time and temperature were recorded. Wide-angle X-ray diffraction (WAXD) data were collected by using the BL17A1 wiggler beamline of the National Synchrotron Radiation Research Center (NSRRC), Taiwan. A triangular bent Si (111) single crystal was employed to obtain a monochromatic beam having a wavelength (λ) of 1.33001 \AA . Transmission electron microscopy (TEM) was performed using a JEOL-2100 electron microscope

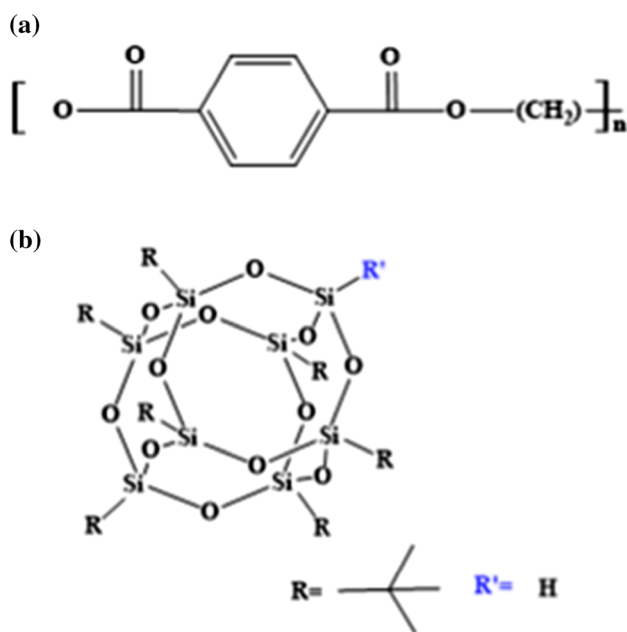


Figure 1 Molecular structure of **a** PET and **b** POSS.

operated at 200 kV. Ultrathin sections (thickness: 700 Å) of the PET and PET/POSS nanocomposites were prepared at room temperature using a Leica Ultracut S microtome equipped with a diamond knife. The ultrathin samples were placed onto a Cu grid, which was coated with a carbon supporting film, without further staining. The crystallization morphologies of PET/POSS were determined with polarized optical microscopy (POM) using Olympus Limited Co. (Japan) with an automatic thermal control hot-stage (Mettler FP90) and were photographed with a CCD camera. The samples were cut and fixed between two thin glass slides and then melt into a film. The samples were melted at 280 °C for 5 min and then cooled to room temperature at the cooling rate of 12 °C min⁻¹ for crystallization.

Results and discussion

Crystallization behavior and morphology of PET with monosilane isobutyl-POSS

Pristine PET is a well-known semicrystallization polymer with the character of a low crystallization rate. It is necessary to improve its crystallization rate in order to use it as an engineering polymer. Incorporation of fillers can effectively affect the crystallization behaviors of the polymer matrix. The melting and crystallization behaviors of PET with POSS are shown in Fig. 2. We can see that the melting peak

temperature has no remarkable shift. Two indistinguishable melting peaks can be observed (Fig. 2a). It is well known that the melting behavior is closely related to crystallization behavior of the polymers. The DSC cooling curves of the PET and PET/POSS nanocomposites are shown in Fig. 2b. The occurrence of two obvious crystallization peaks was observed, suggesting that POSS significantly influenced the crystallization process of PET.

When 0.5 wt% POSS was added, the observed lower crystallization peak temperature (179.1 °C) was even lower than pure PET (191.4 °C), which suggested that a part of the polymer chain segments mobility of PET matrix was restricted. This would indicate there must be a part of the molecularly dispersed POSS acting as a physical cross-link between polymer chains [19]. Moreover, the observed higher crystallization peak temperature (202.6 °C) was higher than pure PET (191.4 °C) when 0.5 wt% POSS was added. Hence, the aggregated POSS in the system acts as nucleating agent to form crystal nuclei during the cooling PET melt. Similar results are also observed in other systems [14, 20]. The dispersion conditions of POSS in the PET system were investigated in the following part. Bruce X. Fu et al. [21] also reported POSS could either enhance crystallization by aggregated POSS or retard crystallization due to dispersed POSS molecules, depending on its concentration and dispersion in the system. Besides, the intensity of the lower crystallization peak increased with increasing the content of POSS. It is believed

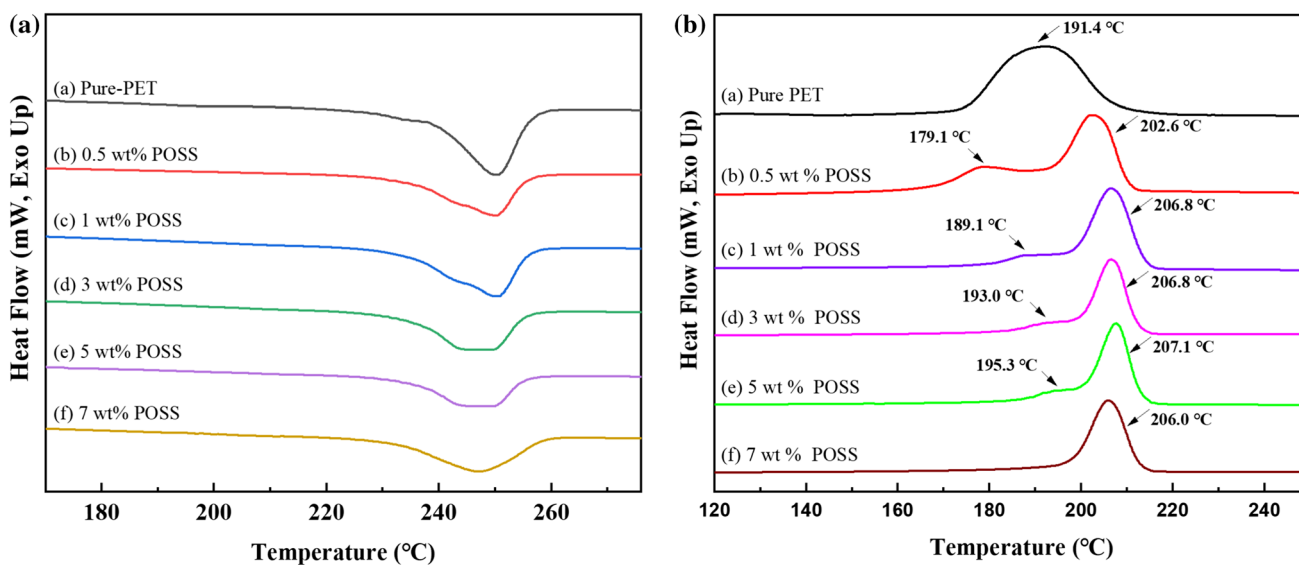
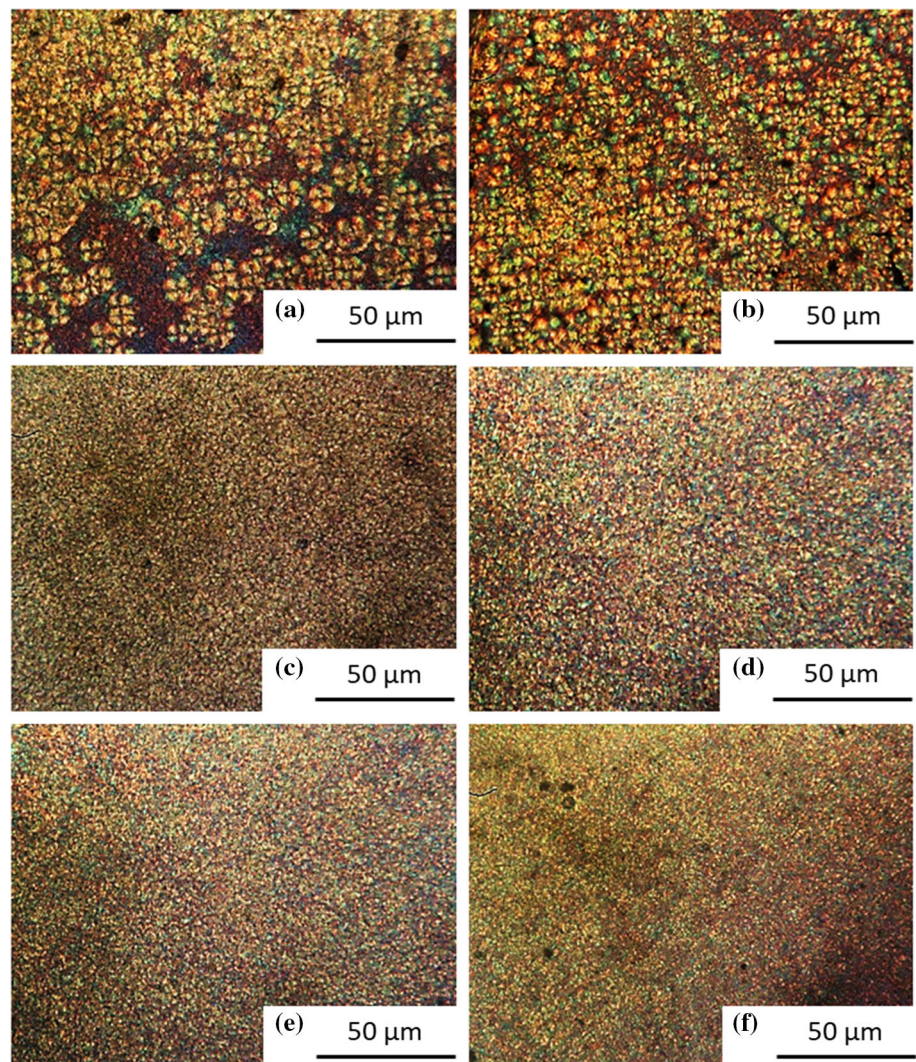


Figure 2 DSC curves for second **a** heating and **b** cooling of PET and PET/POSS nanocomposites with different contents of POSS.

that this phenomenon is caused by the well-dispersed POSS gradual aggregating and acting as a nucleating agent in PET. When the concentration of POSS elevated, the two peak crystallization temperatures gradually increased, which indicated that higher POSS content results in faster rates of crystallization of PET. It is clear that the crystallization peak temperature increased to 206.0 °C from 191.4 °C when PET/POSS nanocomposites contain 7 wt% POSS. For semicrystallization polymer materials, the values of crystallization peak temperature are the indicators for the crystallization rate of polymer in industry. The increased crystallization peak temperature reflected the crystallization happened much easier for the PET/POSS system. Therefore, POSS under higher concentration can act as an effective nucleating agent causing heterogeneous nucleation in the PET system.

While the results of DSC provided the overall behavior of the nanocomposites at a larger length scale, the polarized optical microscopy (POM) could offer information about the shape and size of the crystals. To further confirm the effect of POSS on the crystallization behaviors of PET, the samples were studied with POM. The crystalline morphologies of PET with different contents of POSS are displayed in Fig. 3. The pure PET exhibited rather large spherulites with an average diameter of 10 μm after crystallization completion. The size of spherulites was rather big compared with PET/POSS nanocomposites. The addition of POSS increased the number of crystals as expected. The sample exhibited smaller crystals sizes and higher nucleation densities. With the content of POSS increased, the size of spherulites gradually decreased and the nucleation density

Figure 3 POM pictures of **a** PET, **b** PET/POSS-0.5, **c** PET/POSS-1, **d** PET/POSS-3, **e** PET/POSS-5, **f** PET/POSS-7 after non-isothermally crystallization from 280 to 50 °C at the cooling rate of 12 °C min^{-1} .



gradually increased, indicating that PET crystals were more compact in the system. The reason for this phenomenon is that the spherulites tend to impinge on their neighbors and stop further growth, resulting in smaller spherulites [22]. Overall, the observed improvement of the nucleation density by POM is related to the nucleating ability of POSS and acceleration of the crystallization process, as evidenced by DSC (Fig. 2).

Dispersion of monosilane isobutyl-POSS in PET matrix

The crystallization behaviors of the polymer matrix are closely related to the morphology and distribution of the fillers. Figure 4a–c shows the dispersion

conditions of POSS in the PET system evaluated by transmission electron microscopy (TEM) analysis. It can be observed as dark round images due to the high electron density of the POSS particles [18]. The results indicated that POSS nanoparticles dispersed mostly at the nanometer scale throughout the PET matrix. At lower concentrations, there existed well-dispersed POSS with a diameter of about 3–5 nm, which is close to the original size of POSS particles, but there still existed aggregated particles. At higher concentrations, the particles tended to aggregate to large particles. The phenomenon was consistent with the discussed results above.

The crystal structures of the PET as well as dispersion conditions of POSS in the PET matrix were investigated with wide-angle X-ray diffraction

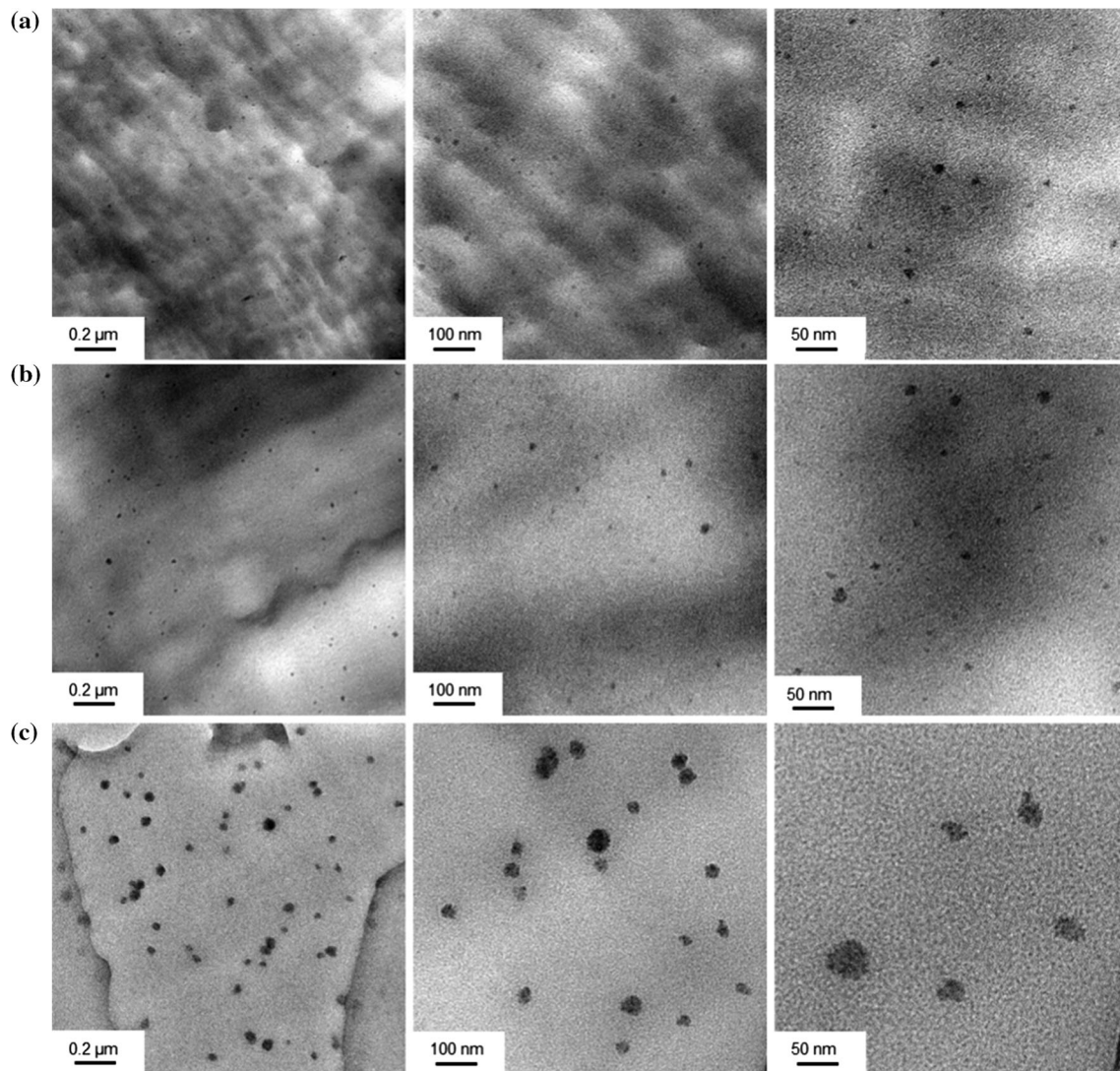


Figure 4 TEM pictures of the PET with the content **a** 0.5 wt %, **b** 3 wt %, and **c** 7 wt % POSS.

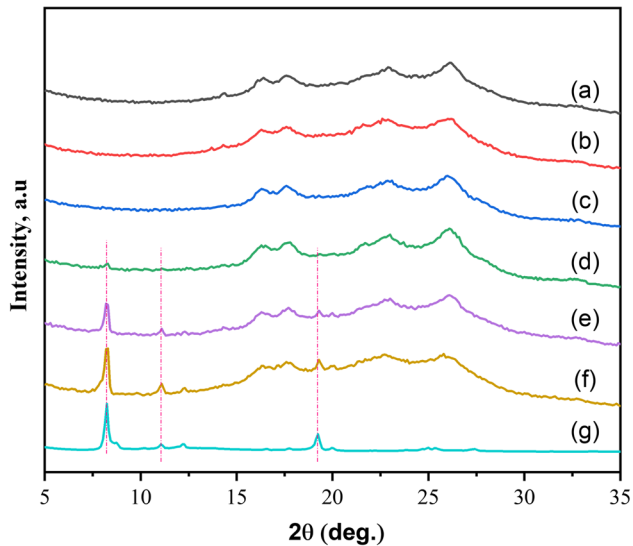


Figure 5 XRD patterns of (a) PET, (b) PET/POSS-0.5, (c) PET/POSS-1, (d) PET/POSS-3, (e) PET/POSS-5, (f) PET/POSS-7, and (g) pure monosilane isobutyl-POSS.

(WAXD). The WAXD patterns for PET and PET/POSS nanocomposites are shown in Fig. 5. The characteristic diffraction peaks of PET revealed at 16.4° (011), 17.6° (010), 21.5° (111), 22.9° (110), and 26.1° (100) as reported before [20]. As for PET/POSS nanocomposites, the characteristic peaks were observed around the same positions, revealing that POSS as an effective heterogeneous nucleating agent did not alter the crystal structure of PET. Besides, the X-ray results of POSS peak positions can be found at 2θ angles of 8.2° , 11.1° , 12.3° , 19.2° as shown in Fig. 5g. We can see that the characteristic peak of POSS could not be observed when the content of POSS was small (Fig. 5b–c), which suggested that the POSS had good dispersion in the PET system under the low concentration. When the content of POSS was increased, the intensity of the characteristic peak of POSS gradually increased (Fig. 5d–f), which indicated the POSS could aggregate to large particles. The results are consistent with the results of the micrographs of TEM (Fig. 4).

Non-isothermal crystallization kinetics of PET with monosilane isobutyl-POSS

The actual process is usually carried out under non-isothermal crystallization conditions in the industry. Therefore, it is necessary to evaluate the non-isothermal crystallization process. As described above, POSS under appropriate concentration acted as an effective nucleating agent to accelerate the

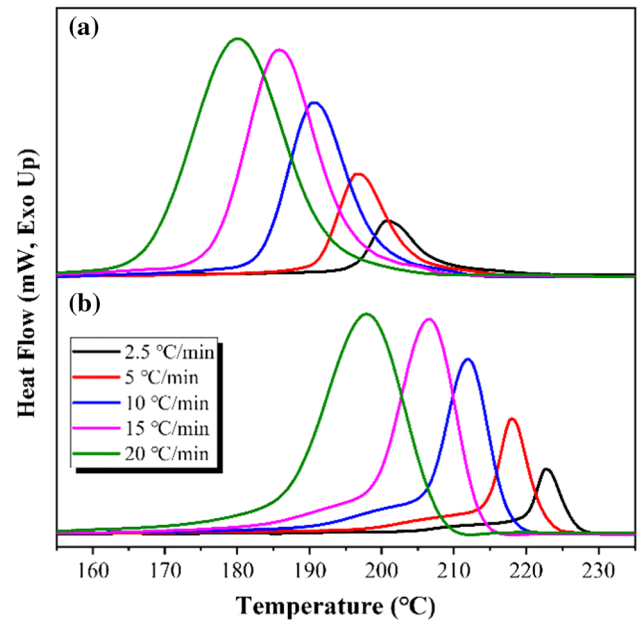


Figure 6 Non-isothermal crystallization exotherms of **a** pure PET and **b** PET/POSS nanocomposites (containing 7 wt% POSS) at different cooling rates.

crystallization process of PET. Therefore, the crystallization kinetics of PET/POSS nanocomposites were further evaluated when 7 wt% POSS added.

As shown in Fig. 6, the non-crystallization behaviors of PET and PET/POSS nanocomposites were investigated with cooling rates from 2.5 to $20\text{ }^\circ\text{C}\cdot\text{min}^{-1}$. As the cooling rate increased, the crystallization peak temperature (T_p) decreased and the curve became flatter, which attributed to the fact that the crystals have less time to nucleate and grow due to the hysteresis as the cooling rate increased

Table 1 Crystallization parameters of pure PET and the PET/POSS nanocomposites (containing 7 wt% POSS)

Samples	R ($^\circ\text{C}\ \text{min}^{-1}$)	T_0 ($^\circ\text{C}$)	T_p ($^\circ\text{C}$)	$t_{1/2}$ (min)
Pure PET	2.5	196.3	200.7	1.57
	5	191.2	196.5	2.19
	10	183.4	190.7	3.38
	15	176.9	185.8	5.63
	20	168.9	180.1	10.25
PET/POSS	2.5	217.4	223	0.77
	5	212.2	218.3	0.88
	10	205	211.9	2.32
	15	198.6	206.6	2.13
	20	187	198	3.12

[23]. As expected, it can be observed that the T_p of PET/POSS nanocomposites is much higher than that of pure PET at equivalent cooling rates, which can be attributed to heterogeneous nucleating effect of POSS in the PET matrix. Table 1 reveals that the crystallization peak temperatures (T_p) were 200.7, 196.5, 190.7, 185.8, and 180.1 °C for pure PET at cooling rates of 2.5, 5, 10, 15, and 20 °C min⁻¹, respectively. The T_p of PET/POSS nanocomposites were 223.0, 218.3, 211.9, 206.6, and 198.0 °C, respectively. The results clearly indicated incorporation of POSS successfully accelerated the crystallization of the PET system at non-isothermal conditions.

The relative crystallization as a function of temperature can be defined as:

$$X(t) = \frac{\int_{t_0}^t (dHc/dt)dt}{\int_{t_0}^{\infty} (dHc/dt)dt} \tag{1}$$

where dHc represents the measured enthalpy of crystallization for an infinitesimal time interval dt at a crystallization temperature (T_c). The relative crystallinity (X_t) curves are shown in Fig. 7. It is clearly indicated the samples of PET/POSS nanocomposites needed less time to completely crystallize. If $X_t = 0.5$, then time is denoted as $t_{1/2}$, which is half-time of crystallization [24]. As listed in Table 1, the values of $t_{1/2}$ for PET and PET/POSS nanocomposites increased with increasing cooling rates due to the thermal hysteresis. Besides, the results showed that the $t_{1/2}$ of PET/POSS nanocomposites was lower

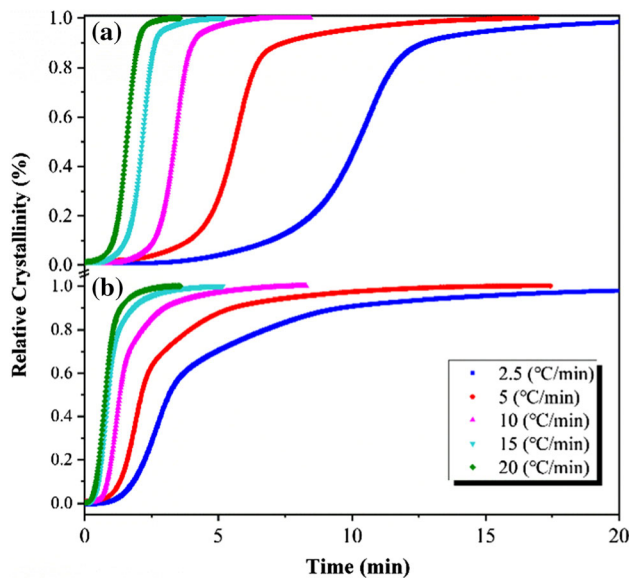


Figure 7 Relative crystallinity of **a** PET and **b** PET/POSS composites as a function of time.

than that of the pure PET system at a given cooling rate, which related to the strong heterogeneous nucleation effect of the POSS in PET system.

Herein, Mo’s model [25] was used to describe the non-isothermal crystallization kinetics. It combined the Avrami equation and the Ozawa equation. At a given crystallinity (X_t), both the Ozawa and the Avrami equations can be expressed as:

$$\log(Z_t) + n \log t = \log K(T) - m \log R \tag{2}$$

And by rearrangement:

$$\log R = \log F(T) - a \log t \tag{3}$$

where $F(T) = (K(T)/Z_t)^{1/m}$ is the cooling rate needed to reach a particular crystallinity at unit crystallization time; a is the ratio of the Avrami exponent, n is the Ozawa exponent, and t is crystallization time [26]. As shown in Fig. 8, the good linearity of plots of $\log R$ and $\log t$ indicated that the equation properly describes the non-isothermal crystallization behavior. The kinetic parameters a and $F(T)$ are determined from the slope and the intercept of the line, respectively. Table 2 lists the values of a and $F(T)$ of PET and PET/POSS nanocomposites under different X_t . The values of a change slightly with X_t , as seen from Table 2. It is observed that the values of

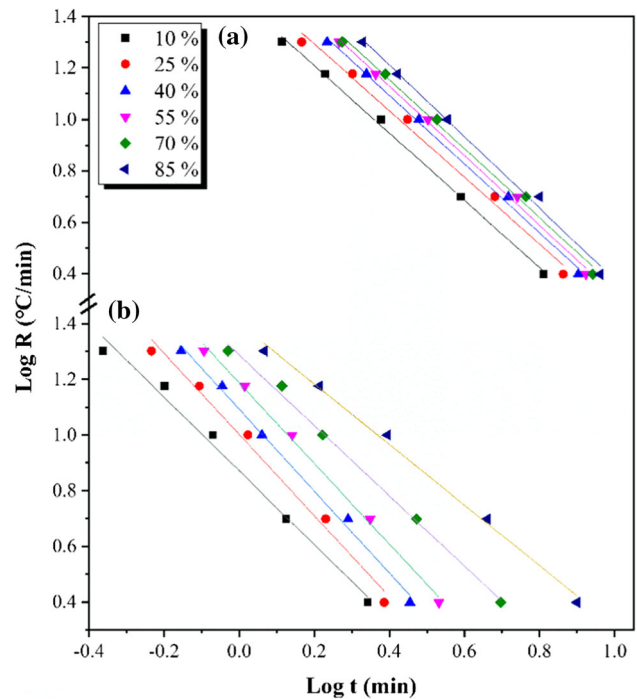


Figure 8 Plots of $\log R$ versus $\log t$ for non-isothermal crystallization of **a** PET and **b** PET/POSS composites.

Table 2 Crystallization kinetic parameters of pure PET and the PET/POSS nanocomposites

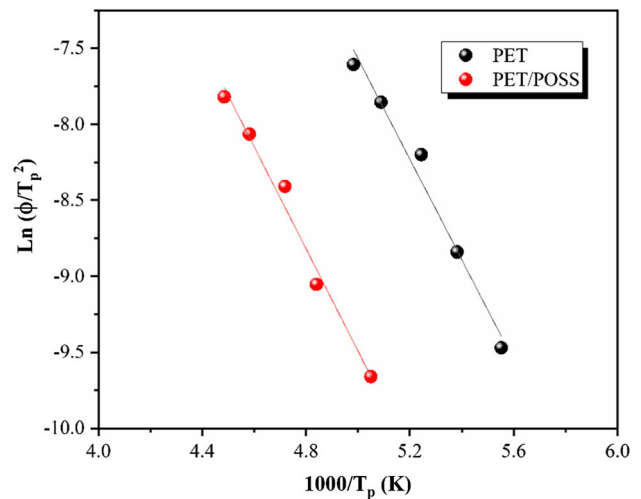
Samples	X_t (%)	a	$F(T)$
Pure PET	10	1.19	25.17
	25	1.18	30.49
	40	1.21	36.1
	55	1.23	39.75
	70	1.22	41.68
	85	1.26	49.43
PET/POSS	10	1.32	7.43
	25	1.46	10.05
	40	1.47	12.39
	55	1.45	15.4
	70	1.26	19.38
	85	1.09	25.2

$F(T)$ gradually increased with increasing X_t , which suggested a higher cooling rate was required to reach a particular crystallinity under unit crystallization time. Also, it can be seen that the values of $F(T)$ for the pure PET were lower than PET/POSS nanocomposites under the same X_t . A lower value of $F(T)$ implies that the crystallization time for PET/POSS nanocomposites was shorter to reach the same X_t and the crystallization process was much easier [27]. Overall, this result indicated the POSS nanoparticles contributed to increasing the overall crystallization rate of PET, which is consistent with the data above.

To further study the difference between pure PET and PET/POSS nanocomposites, the evolution of the crystallization activation energy (ΔE) for the samples was investigated using the method of Kissinger. According to the method, ΔE can be calculated as the following expression:

$$d\ln(\Phi/T_p^2)/d(1/T_p) = -\Delta E/R \quad (4)$$

where Φ represents the cooling rate, T_p is the crystallization peak temperature, and R is the gas constant. Plotting $\ln(\Phi/T_p^2)$ against $1/T_p$, the activation energy (ΔE) can be obtained from the slope. The linear behavior between $\ln(\Phi/T_p^2)$ and $1/T_p$ indicated the method is suitable for describing the activation energy of pure PET and PET/POSS nanocomposites during the non-isothermal crystallization process, as shown in Fig. 9. The ΔE values of the pure PET increased from 27.5 to 27.9 kJ mol⁻¹ after introducing POSS. The results can be analyzed

**Figure 9** Kissinger plots for calculating the non-isothermal crystallization activation energy for pure PET and PET/POSS nanocomposites.

from the view of the crystallization process of polymers, which includes nucleation and crystal growth processes. Herein, the incorporation of POSS improved the nucleation process of PET, which induces the movement of PET chains to initially form a partially crystalline phase. Therefore, the nucleation process is much rapid for the PET/POSS composites. Then, the crystalline phase hindered the movement of random PET chains due to entanglement [28], leading to the absolute value of activation energy increasing. Therefore, increasing ΔE can be observed when POSS is added. Similar results were reported for the nucleating agents in other systems by several researchers [28–33]. In conclusion, the POSS nanoparticles improved the crystallization of PET through accelerating of the nucleation process.

Isothermal crystallization kinetics of PET with monosilane isobutyl-POSS

Figure 10 illustrates the isothermal crystallization behavior of PET and PET/POSS nanocomposites at various temperatures. It can be seen that the exothermic curves became wider and it took more time to complete the crystallization with increasing crystallization temperature (T_c). The phenomenon indicated crystallization process slowed down with T_c increased. It is reasonable because the degree of supercooling decreased with higher T_c , leading to the weaker driving force for PET crystallization [24, 34]. Besides, the crystallization process of PET/POSS

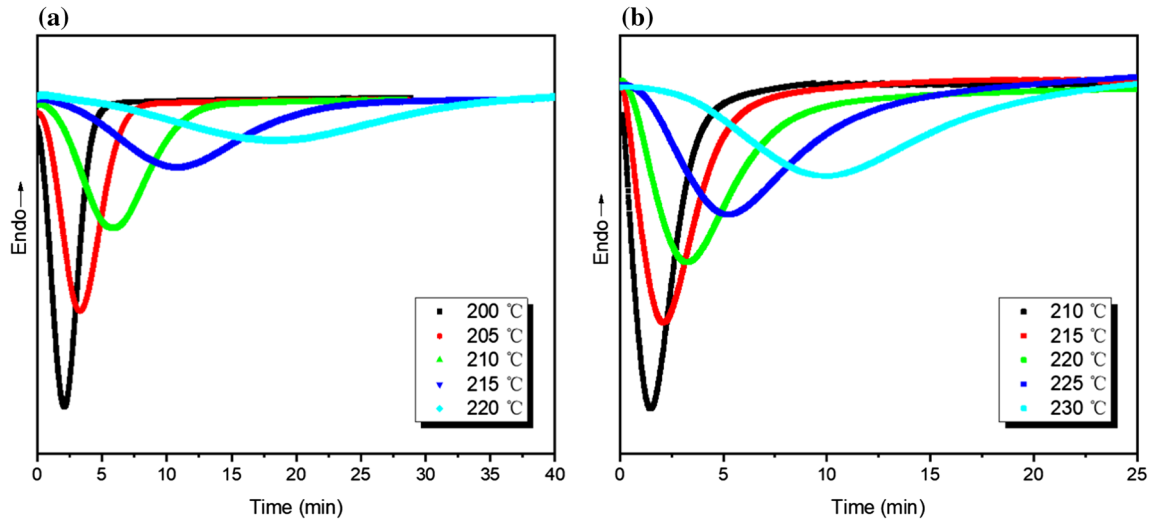


Figure 10 Crystallization exothermic curves for **a** PET and **b** PET/POSS nanocomposites (containing 7 wt% POSS).

nanocomposites could begin at higher temperatures than pure PET; therefore, it can be understood that the overall crystallization kinetics were promoted under the practical process. Figure 11a–b shows the plots of relative crystallinity against crystallization time at different crystallization temperatures for PET and PET/POSS nanocomposites. At the same isothermal crystallization temperature (T_c), such as 220 °C, it took pure PET nearly 40 min to complete the crystallization process, while PET/POSS finished it within 20 min. The results showed POSS can act as a nucleating agent producing nucleating sites in the PET matrix, resulting in dramatically accelerating the isothermal crystallization process.

To get a better insight into the influence of POSS on the crystallization behavior of PET, the classic Avrami equation was employed to analyze the isothermal crystallization kinetics, which has been reported to successfully describe the isothermal crystallization kinetics of PET with nanoparticles [24]. The Avrami equation assumes that relative crystallinity (X_t) develops as crystallization time (t), which can be expressed as:

$$1 - X_t = e^{(-kt^n)} \quad (5)$$

where k is the crystallization rate constant involving nucleation and growth rate parameters and n is the Avrami exponent that depended on the nucleation and growth geometry of the crystals [12]. The plots of $\log\{-\ln[1-X_t]\}$ versus $\log t$ for neat PET and PET/POSS at different crystallization temperatures are depicted in Fig. 11c–d. We can see the fitting lines

were almost parallel straight line and the linear correlation coefficients were all above 0.99, which indicated the Avrami equation is suitable to describe the overall isothermal crystallization behavior for pure PET and PET/POSS nanocomposite. The values of n and k can be calculated from the slopes and intercepts of the Avrami plots, as summarized in Table 3. The average value of n over all values of T_c was 2.58 ± 0.3 for PET and 2.74 ± 0.22 for PET/POSS, which indicated that the growth of spherulite was a three-dimensional growth process. The values of n for PET were very close to that of the PET/POSS nanocomposites, indicating that the spherulite growth patterns of PET did not change with the addition of POSS. Similar results of n values are reported elsewhere [12, 24].

The plots of $1/t_{1/2}$ versus T_c for pure PET and PET/POSS nanocomposites are illustrated in Fig. 12. The sample of PET/POSS nanocomposites can complete the crystallization with higher temperature and less time, suggesting that POSS have a positive influence on the isothermal crystallization process. For example, $t_{1/2}$ of PET/POSS was 69% shorter than that of pure PET at 210 °C and 77% shorter at 220 °C. Compared to pure PET, PET/POSS nanocomposites crystallized much faster. At the same crystallization temperature, the crystallization completion time of PET/POSS nanocomposites was shorter. These results indicated again that the POSS was an effective nucleating agent for the crystallization process of the PET matrix and successfully accelerated the crystallization process.

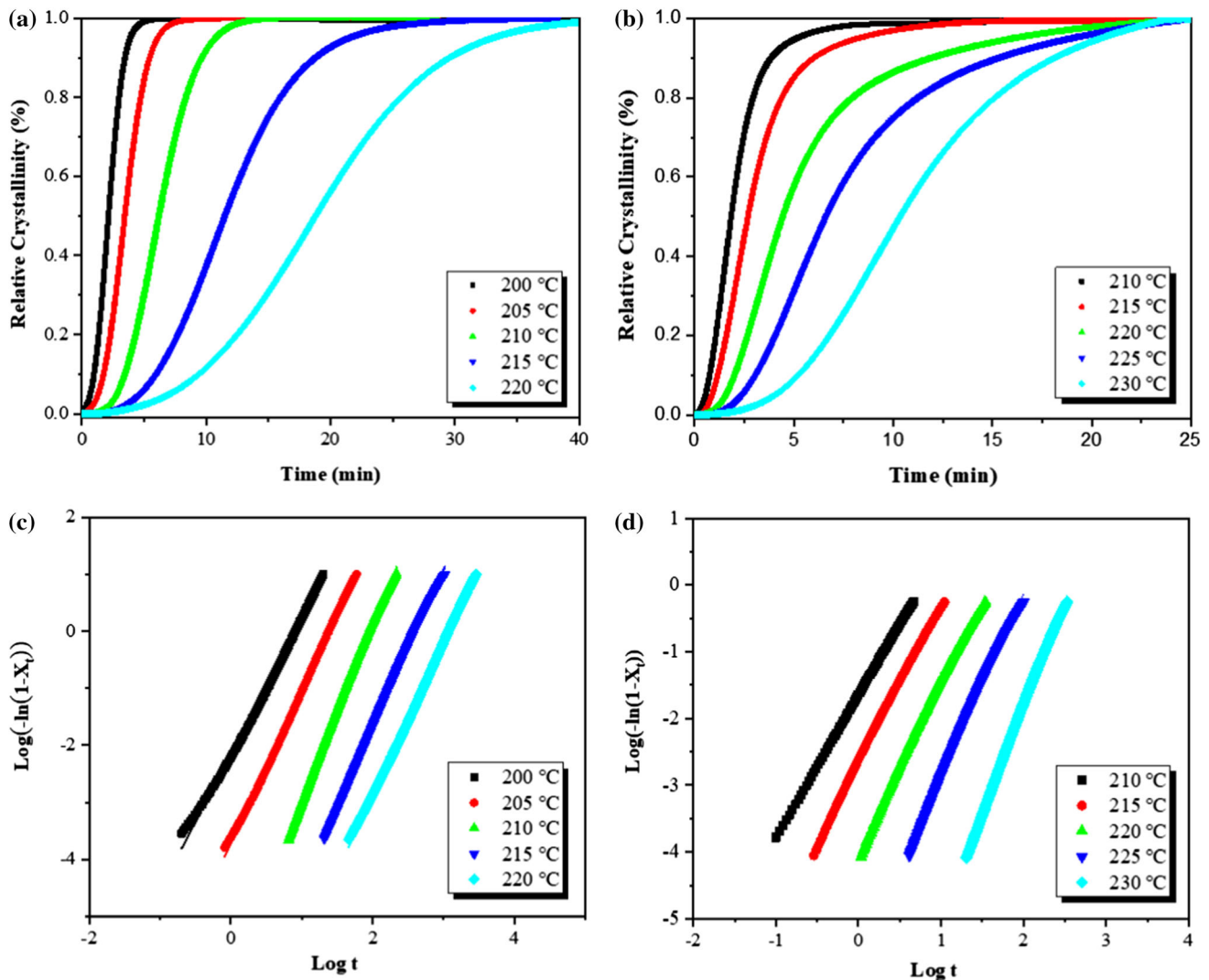


Figure 11 Plots of relative crystallinity against crystallization time for **a** pure PET and **b** PET/ POSS, and plots of $\log\{-\ln[1 - X_t]\}$ vs. $\log t$ for **c** neat PET and **d** PET/POSS at different crystallization temperatures.

Table 3 Summary of the Avrami Parameters for pure PET and PET/POSS

Samples	T_c (°C)	n	K (min $^{-n}$)	$t_{1/2}$ (min)
Pure PET	200	2.2	$2.2 \cdot 10^{-2}$	1.88
	205	2.4	$2.2 \cdot 10^{-3}$	3.08
	210	2.5	$1.0 \cdot 10^{-4}$	5.92
	215	2.7	$2.7 \cdot 10^{-6}$	11.58
	220	3.1	$6.7 \cdot 10^{-9}$	18.95
PET/POSS	210	2.4	$6.9 \cdot 10^{-3}$	1.85
	215	2.7	$2.2 \cdot 10^{-4}$	2.68
	220	3.1	$9.9 \cdot 10^{-7}$	4.42
	225	2.8	$6.5 \cdot 10^{-8}$	7.03
	230	2.7	$6.1 \cdot 10^{-9}$	11.95

Conclusions

In the present work, the PET/monosilane isobutyl-POSS blends were prepared and the crystallization behavior, morphology, crystal structure, non-isothermal, and isothermal crystallization kinetics were investigated. Two obvious crystallization peaks were observed when the content of POSS was small and the peak shift to higher temperatures as the content of POSS increased. Overall, the experimental results clearly showed that POSS under appropriate concentration can effectively improve the crystallization temperature of the PET and improved its nucleation efficiency. The POSS particles are mostly at the nanometer scale in the PET matrix as

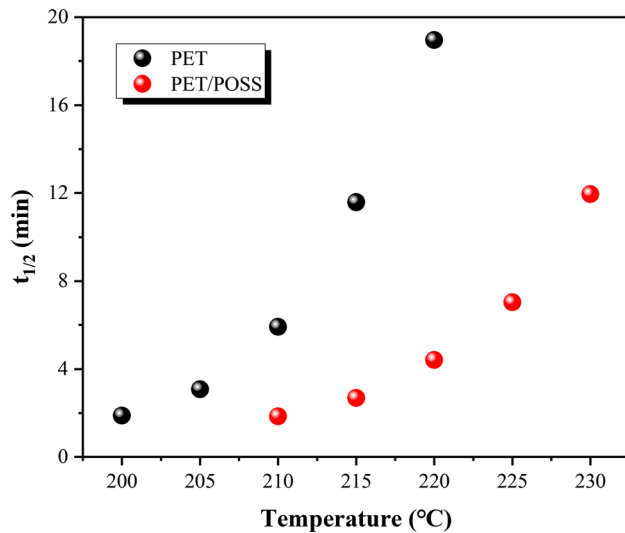


Figure 12 $t_{1/2}$ of pure PET and PET/POSS nanocomposites under isothermal crystallization at different temperatures.

determined by TEM. At higher concentrations, the particles tended to aggregate into large particles. Besides, POM micrographs showed that the nucleation density gradually increased as the content of POSS increased, indicating the nucleating ability of POSS and acceleration of the crystallization process. Furthermore, Mo's method was successful in describing the non-isothermal crystallization process of PET and the PET/POSS nanocomposites (containing 7 wt% POSS). PET/POSS nanocomposites provided smaller $F(T)$ values than pure PET, suggesting that the cooling rate required to attain a relative crystallinity at a given time was less than that of pure PET. Moreover, the isothermal crystallization process of PET/POSS nanocomposites could happen at higher temperature and need less time to complete crystallization than pure PET; therefore, it can be understood that the overall crystallization kinetics were promoted under the practical process.

Acknowledgements

This work was financially supported by National Natural Science Foundation of China (Grants 21878089 and 21606084), the National Key R&D Program of China (2016YFB0302201), the Fundamental Research Funds for the Central Universities (22221818010), and the National Natural Science Funds of China (Grant No. 21776079).

Compliance with ethical standards

Conflict of interest The authors declare that they have no known competing financial interests or personal relationships that could have appeared to influence the work reported in this paper.

References

- [1] Xing S, Li R, Si J, Tang P (2016) In situ polymerization of poly(styrene-alt-maleic anhydride)/organic montmorillonite nanocomposites and their ionomers as crystallization nucleating agents for poly(ethylene terephthalate). *J Ind Eng Chem* 38:167–174. <https://doi.org/10.1016/j.jiec.2016.04.020>
- [2] Kim K, Kashani Rahimi S, Alam TM, Sorte EG, Otaigbe JU (2018) Unexpected effects of inorganic phosphate glass on crystallization and thermo-rheological behavior of polyethylene terephthalate. *Polymer* 154:135–147. <https://doi.org/10.1016/j.polymer.2018.08.066>
- [3] Jiang XL, Luo SJ, Sun K, Chen XD (2007) Effect of nucleating agents on crystallization kinetics of PET. *Express Polym Lett* 1(4):245–251. <https://doi.org/10.3144/expresspolymlett.2007.37>
- [4] Chuah HH (2001) Crystallization kinetics of poly(trimethylene terephthalate). *Polym Eng Sci* 41(2):308–313. <https://doi.org/10.1002/pen.10730>
- [5] Dong F, Lu L, Ha CS (2019) Silsesquioxane-containing hybrid nanomaterials: fascinating platforms for advanced applications. *Chem Phys Macromol*. <https://doi.org/10.1002/macp.201800324>
- [6] Mohamed MG, Kuo S-W (2016) Polybenzoxazine/polyhedral oligomeric silsesquioxane (POSS) nanocomposites. *Polymers*. 8(225):12. <https://doi.org/10.3390/polym8060225>
- [7] Laine ASRM (1996) Silsesquioxanes as synthetic platforms. thermally curable and photocurable inorganic/organic hybrids. *Macromolecules* 29:2327–2330. <https://doi.org/10.1021/ma951499y>
- [8] Kuo S-W, Chang F-C (2011) POSS related polymer nanocomposites. *Prog Polym Sci* 36(12):1649–1696. <https://doi.org/10.1016/j.progpolymsci.2011.05.002>
- [9] Raftopoulos KN, Pielichowski K (2016) Segmental dynamics in hybrid polymer/POSS nanomaterials. *Prog Polym Sci* 52:136–187. <https://doi.org/10.1016/j.progpolymsci.2015.01.003>
- [10] Zhao Y, Schiraldi DA (2005) Thermal and mechanical properties of polyhedral oligomeric silsesquioxane (POSS)/polycarbonate composites. *Polymer* 46(25):11640–11647. <https://doi.org/10.1016/j.polymer.2005.09.070>

- [11] Yang H, Caydamli Y, Fang X, Tonelli AE (2015) Crystallization behaviors of modified poly (ethylene terephthalate) and their self-nucleation ability. *Macromol Mater Eng* 300(4):403–413. <https://doi.org/10.1002/mame.201400348>
- [12] Teng S, Qiu Z (2017) Nucleating and plasticization effects of low-loading octavinyl-polyhedral oligomeric silsesquioxanes in novel biodegradable poly(ethylene succinate-co-diethylene glycol succinate)-based nanocomposite. *Ind Eng Chem Res* 56(50):14807–14813. <https://doi.org/10.1021/acs.iecr.7b04004>
- [13] Chen K, Yu J, Qiu Z (2013) Effect of low octavinyl-polyhedral oligomeric silsesquioxanes loading on the crystallization kinetics and morphology of biodegradable poly(ethylene succinate-co-5.1 mol % ethylene adipate) as an efficient nucleating agent. *Indust Eng Chem Res* 52(4):1769–1774. <https://doi.org/10.1021/ie303510h>
- [14] Chen J-H, Chiou Y-D (2006) Crystallization behavior and morphological development of isotactic polypropylene blended with nanostructured polyhedral oligomeric silsesquioxane molecules. *J Polym Sci Part B Polym Phys* 44(15):2122–2134. <https://doi.org/10.1002/polb.20878>
- [15] Zeng J, Kumar S, Iyer S, Schiraldi D, Gonzalez R (2005) Reinforcement of poly(ethylene terephthalate) fibers with polyhedral oligomeric silsesquioxanes (POSS). *High Perform Polym* 17:403–424. <https://doi.org/10.1177/0954008305055562>
- [16] Vannier A, Duquesne S, Bourbigot S, Alongi J, Camino G, Delobel R (2009) Investigation of the thermal degradation of PET, zinc phosphinate, OMPOSS and their blends—identification of the formed species. *Thermochim Acta* 495(1–2):155–166. <https://doi.org/10.1016/j.tca.2009.06.013>
- [17] Lee AS, Jeon H, Choi S-S, Park J, Hwang SY, Jegal J, Oh DX, Kim BC, Hwang SS (2017) Crystallization derivation of amine functionalized T12 polyhedral oligomeric silsesquioxane-conjugated poly(ethylene terephthalate). *Compos Sci Technol* 146:42–48. <https://doi.org/10.1016/j.compscitech.2017.04.015>
- [18] Sirin H, Turan D, Ozkoc G, Gurdag S (2013) POSS reinforced PET based composite fibers: “Effect of POSS type and loading level”. *Compos B Eng* 53:395–403. <https://doi.org/10.1016/j.compositesb.2013.05.033>
- [19] Milliman HW, Ishida H, Schiraldi DA (2012) Structure property relationships and the role of processing in the reinforcement of nylon 6-POSS blends. *Macromolecules* 45(11):4650–4657. <https://doi.org/10.1021/ma3002214>
- [20] Yan Y, Gooneie A, Ye H, Deng L, Qiu Z, Reifler FA, Hufenus R (2018) Morphology and crystallization of bio-based polyamide 56 blended with polyethylene terephthalate. *Macromol Mater Eng*. <https://doi.org/10.1002/mame.201800214>
- [21] Fu BX, Yang L, Somani RH, Zong SX, Hsiao BS, Phillips S, Blanski R, Ruth P (2001) Crystallization studies of isotactic polypropylene containing nanostructured polyhedral oligomeric silsesquioxane molecules under quiescent and shear conditions. *J Polym Sci Part B Polym Phys* 39(22):2727–2739. <https://doi.org/10.1002/polb.10028>
- [22] Jiang X, Zhang W, Zhao S, Zhou S, Shi Y, Xin Z (2018) Effect of benzoic acid surface modified alumina nanoparticles on the mechanical properties and crystallization behavior of isotactic polypropylene nanocomposites. *RSC Adv* 8(37):20790–20800. <https://doi.org/10.1039/c8ra01069b>
- [23] Zhang Z, Feng L, Li Y, Wang Y, Yan C (2015) Non-isothermal crystallization kinetics of poly(butylene terephthalate)/poly(ethylene terephthalate)/glass fiber composites. *Polym Compos* 36(3):510–516. <https://doi.org/10.1002/pc.22966>
- [24] Nikam PN, Deshpande VD (2019) Isothermal crystallization kinetics of PET/alumina nanocomposites using distinct macrokinetic models. *J Therm Anal Calorim* 138(2):1049–1067. <https://doi.org/10.1007/s10973-019-08192-x>
- [25] Zhishen M (2008) A method for the non-isothermal crystallization kinetics of polymers. *Acta Polym Sin* 7(7):656–671. <https://doi.org/10.3724/SP.J.1105.2008.00656>
- [26] Gao J, Cao X, Zhang C, Hu W (2013) Non-isothermal crystallization kinetics of polypropylene/MAP-POSS nanocomposites. *Polym Bull* 70(7):1977–1990. <https://doi.org/10.1007/s00289-013-0907-2>
- [27] Rasana N, Jayanarayanan K, Pegoretti A (2018) Non-isothermal crystallization kinetics of polypropylene/short glass fibre/multiwalled carbon nanotube composites. *RSC Adv* 8(68):39127–39139. <https://doi.org/10.1039/c8ra07243d>
- [28] Meng X, Gong W, Chen W, Shi Y, Sheng Y, Zhu S, Xin Z (2018) Isothermal and non-isothermal crystallization of isotactic polypropylene in the presence of an α nucleating agent and zeolite 13X. *Acta Thermochim*. <https://doi.org/10.1016/j.tca.2018.03.008>
- [29] Devaux E, C. (1997) A new method to determine the Avrami exponent by dsc studies of non-isothermal crystallization from the molten state. *Polymer* 38(3):497–502. [https://doi.org/10.1016/S0032-3861\(96\)00552-6](https://doi.org/10.1016/S0032-3861(96)00552-6)
- [30] Ma YI, Hu Gs, Ren XI, Wang Bb (2007) Non-isothermal crystallization kinetics and melting behaviors of nylon 11/tetrapod-shaped ZnO whisker (T-ZnOw) composites. *Mater Sci Eng A* 460–461:611–618. <https://doi.org/10.1016/j.msea.2007.01.133>
- [31] Cao L, Zheng A, Cao X, Yuan D, Xu C, Chen Y (2017) Morphology and non-isothermal crystallization of

- dynamically vulcanized PP/EPDM blends in situ compatibilized via magnesium dimethacrylate. *Polym Test* 62:68–78. <https://doi.org/10.1016/j.polymertesting.2017.06.014>
- [32] Zhao S, Xu N, Xin Z, Jiang C (2012) A novel highly efficient β -nucleating agent for isotactic polypropylene. *J Appl Polym Sci* 123(1):108–117. <https://doi.org/10.1002/app.34441>
- [33] Zhao S, Cai Z, Xin Z (2008) A highly active novel β -nucleating agent for isotactic polypropylene. *Polymer* 49(11):2745–2754. <https://doi.org/10.1016/j.polymer.2008.04.012>
- [34] Teng S, Qiu Z (2017) Enhanced crystallization and mechanical properties of biodegradable poly(ethylene succinate) by octaisobutyl-polyhedral oligomeric silsesquioxanes in their nanocomposites. *Thermochim Acta* 649:22–30. <https://doi.org/10.1016/j.tca.2017.01.004>

Publisher's Note Springer Nature remains neutral with regard to jurisdictional claims in published maps and institutional affiliations.